Artificial Neural Network Models for Identifying Flow Regimes and Predicting Liquid Holdup in Horizontal Multiphase Flow

El-Sayed A. Osman, SPE, King Fahd U. of Petroleum and Minerals

Summary

This paper presents two artificial neural network (ANN) models to identify the flow regime and calculate the liquid holdup in horizontal multiphase flow. These models are developed with 199 experimental data sets and with three-layer back-propagation neural networks (BPNs). Superficial gas and liquid velocities, pressure, temperature, and fluid properties are used as inputs to the model. Data were divided into three portions: training, cross validation, and testing. The results show that the developed models provide better predictions and higher accuracy than the empirical correlations developed specifically for these data groups. The developed flow-regime model predicts correctly for more than 97% of the data points. The liquid-holdup model outperforms the published models; it provides holdup predictions with an average absolute percent error of 9.407, a standard deviation of 8.544, and a correlation coefficient of 0.9896.

Introduction

Multiphase flow is defined as the concurrent flow of two or more phases (liquid, solid, or gas) in which the motion influences the interface between the phases. The flow regime or flow pattern is a qualitative description of the phase distribution in the pipe. There are three types of flow regimes in horizontal gas-liquid flow, namely, segregated, intermittent, and distributive flows. Segregated flow is further classified into stratified smooth, stratified wavy, and annular flow regimes. The intermittent flow regimes are slug and plug (elongated bubble) flows. Distributive flow regimes include bubble and mist flows.[1] Other investigators[2] classified flow regimes in horizontal gas-liquid flow as bubble flow (in which gas bubbles tend to float at the top in the liquid), stratified flow (in which the liquid flows along the bottom of the pipe and the gas flows on top), intermittent or slug flow (in which large frothy slugs of liquid alternate with large gas pockets), and annular flow (in which a liquid ring is attached to the pipe wall with gas blowing through). The layer at the bottom is usually much thicker than the one at the top. The flow regimes in horizontal gas-liquid flow are illustrated in **Fig. 1.**

Predicting flow regimes is essential for properly calculating the pressure drop across the pipe under different multiphase flow conditions. Flow-regime maps have been developed and are used to predict flow regimes in horizontal gas-liquid flow. Most are plots of superficial liquid velocity vs. superficial gas velocity. One of the first maps used in the oil industry is that of Baker.[3] Ten years later, it was modified by Scott.[4] Beggs and Brill[5] and Mandhane[6] presented other flow-pattern maps that were constructed based on experimental data. Taitle and Dukler[7] developed a theoretical model for the flow regime transitions in horizontal gas-liquid flow. Recently, other studies have been carried out for the prediction of specific transitions. Separate models have been developed for stratified,[8–10] slug,[11–14] annular,[15–16] and dispersed bubble flows.[17] An example of these flow-pattern maps is given in **Fig. 2.**

Predicting liquid holdup in the pipeline is very important to the petroleum industry. Liquid holdup, defined as the fraction of pipe occupied by liquid, must be predicted to properly design separation equipment and slug catchers in pipeline operations. Many correlations have been published for predicting this important parameter, of which the most commonly used are Eaton and Brown,[18] Guzhov *et al.*,[19] Beggs and Brill,[5] Minami and Brill,[20] Brill *et al.*,[21] Gregory *et al.*,[22] Mukherjee and Brill,[23] Hughmark and Pressburg,[24] Hughmark,[25] Abdul-Majeed,[26,27] Xiao *et al.*,[28] Baker *et al.*,[29] and Gomez *et al.*[30]

This paper presents ANN models for identifying the flow regime and predicting the liquid holdup in horizontal gas-liquid flow. Published experimental data were used to train and test the neural-network models developed. Superficial gas and liquid velocities, pressure, temperature, and fluid properties are used as input to the models. The output of the first model is the flow regime, while the other model predicts the liquid holdup.

ANNs are parallel-distributed information-processing models that can recognize highly complex patterns within available data. In recent years, neural network use has gained popularity in petroleum applications,[31] but few studies were carried out to model multiphase flow using neural networks. Van der Spek and Thomas[32] used neural networks to identify the flow regime with band spectra of flow-generated sound. They concluded that the flow regime can be classified correctly by a neural network in up to 87% of all cases studied with one-third octave band spectra of flow-generated sound plus the pipe inclination angle. Ternyik *et al.*[33] used neural networks to predict the holdup and flow pattern in pipes under various angles of inclinations. They developed neural-network models based on experimental data limited to a 1.5-in. pipe and low operating pressures and a Kohonen-type network to classify the flow patterns with all input data. The resulting classifications were used as data input to another model for predicting holdup. Their model predicted holdup values with a correlation coefficient of 0.945. The other neural-network model developed for flow-pattern prediction was based on slug, bubble, annular mist, and stratified flows. It predicted a minimum of 82.8% (in bubble flow) and a maximum of 93.3% (in slug flow).

Neural Networks

An ANN is a computer model that attempts to mimic simple, biological learning processes and simulate specific functions of the human nervous system. It is an adaptive, parallel, information-processing system able to develop associations, transformations, or mappings between objects or data. It is also the most popular intelligent technique for pattern recognition to date. The basic elements of a neural network are the neurons and their connection strengths (weights). Given a topology of the network structure expressing how the neurons (the processing elements) are connected, a learning algorithm takes an initial model with some previous connection weights (usually random numbers) and produces a final model by numerical iterations. Hence, "learning" implies the derivation of the posterior connection weights when a performance criterion is matched (e.g., the mean square error is less than a certain tolerance value). Learning can be performed by

This paper (SPE 86910) was revised for publication from paper SPE 68219, first presented at the 2001 SPE Middle East Oil Show, Bahrain, 17–20 March. Original manuscript received for review 23 April 2001. Revised manuscript received 4 June 2003. Paper peer approved 27 June 2003.

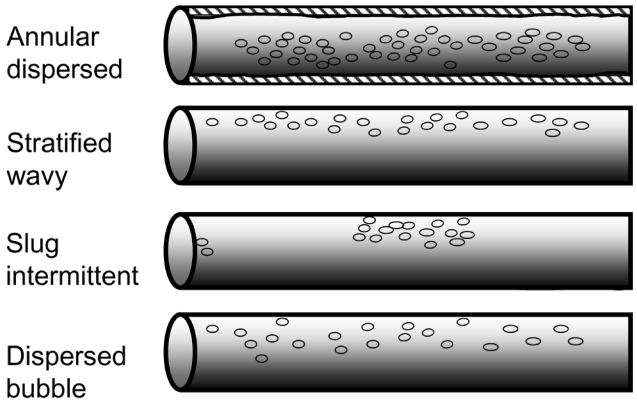

Fig. 1—Different flow regimes in horizontal multiphase flow.

"supervised" or "unsupervised" algorithm. The former requires a set of known input-output data patterns (or training patterns), while the latter needs only the input patterns. This is commonly known as the feed-forward model, in which no lateral or backward connections are used.[34]

Advantages of ANNs. Several advantages can be attributed to ANNs, rendering them suitable for applications such as those considered here. First, an ANN learns the behavior of a database population by self-tuning its parameters in such a way that the trained ANN matches the employed data accurately. Second, if the data used are sufficiently descriptive,[35] the ANN provides a rapid and confident prediction as soon as a new case that has not been seen by the model during the training phase is applied. Possibly the most important aspect of ANNs is their ability to discover patterns in data that are so obscure as to be imperceptible to normal observation and standard statistical methods. This is the case particularly for data exhibiting significantly unpredictable nonlinearities.[36] Traditional correlations are based on simple models that often have to be stretched by adding terms and constants for them to become flexible enough to fit experimental data, whereas neural networks are marvelously self-adaptable.

An ANN model can accept substantially more information as input to the model, thereby significantly improving the accuracy of the predictions and reducing the ambiguity of the requested relationship. Moreover, ANNs are fast-responding systems. Once the model has been educated, predictions about unknown properties are obtained with direct and rapid calculations without the need for tuning or iterative computations. Furthermore, an outstanding attribute of the ANNs is their capability of becoming increasingly expert by retraining them with larger databases. Continuous enrichment of the ANN's knowledge eventually leads to a predictive model that exhibits accuracy comparable to the original data itself.[37]

Neural-Network Architecture

Different neural networks were developed for holdup and flow-pattern predictions. A three-layer BPN was used in all cases because of its success in solving other petroleum engineering problems and its ability to generalize with good accuracy. Finally, two BPNs were used: the first one was designed to predict flow patterns, while the second was constructed to calculate the liquid holdup. A BPN is multilayered, and information flows from the input to the output through at least one hidden/middle layer. Each layer contains neurons connected to all neurons in the neighboring layers. The connections have numerical values (weights) associated with them. During the training phase, the weights are adjusted according to the generalized delta rule. Training is completed when the network is able to predict the given output.

Data Acquisition

Data used for this work are collected from studies carried out by Minami and Brill[20] and Abdul-Majeed.[27] The Minami and Brill data (111 points) were obtained with air-water and air-kerosene mixtures and were used to develop their correlations. According to Mandhane's map,[6] 55 points fell in the stratified-smooth flow region, 26 in the stratified-wavy flow, and 30 in the slug flow. Abdul-Majeed's data (88 points) were obtained with an air-kerosene mixture. Based on Mandhane's flow-pattern map,[6] 20 points were in stratified-smooth flow, 13 in stratified-wavy flow, 33 in slug flow, and 22 in annular flow. Hence, the combined data contain 75 points in the stratified-smooth flow region, 39 in the stratified-wavy flow region, 63 in the slug flow region, and 22 in the annular flow region. Locations of those experimental data and their corresponding flow regimes are plotted on a superficial gas-liquid velocity crossplot (see **Fig. 3**). The 199 data sets were divided into 150 sets for training ANN models, of which 100 sets were used to estimate the weights of the neural network and 50 were for cross validation of the calculated weights during the training phase of the model. The remaining 49 sets were used for testing the developed models. Statistical description of training and test data are given in **Tables 1 and 2,** respectively.

Liquid-Holdup Network. The neural network developed to predict the liquid holdup was based on a design similar to that of the flow regimes (i.e, three-layer BPN). The first layer consists of four neurons representing the input values of temperature, pressure, superficial gas velocity, and superficial liquid velocity. The second (hidden) layer consists of 12 neurons, and the third layer contains one neuron that represents the output value of the liquid holdup. A simplified schematic of the neural network is illustrated in **Fig. 4.**

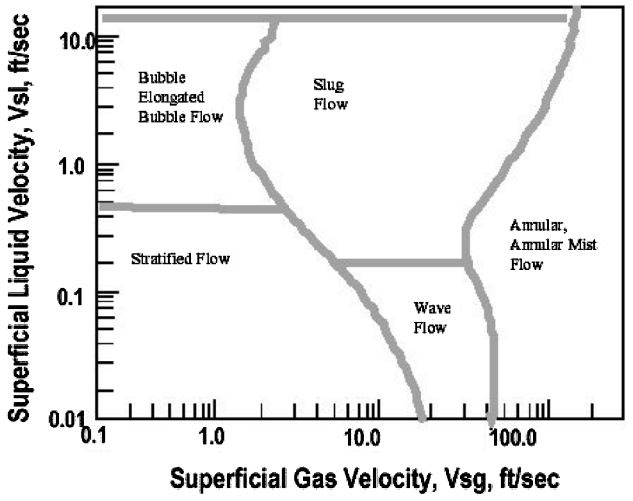

Fig. 2—Horizontal multiphase-flow-pattern map (after Mandhane[6]).

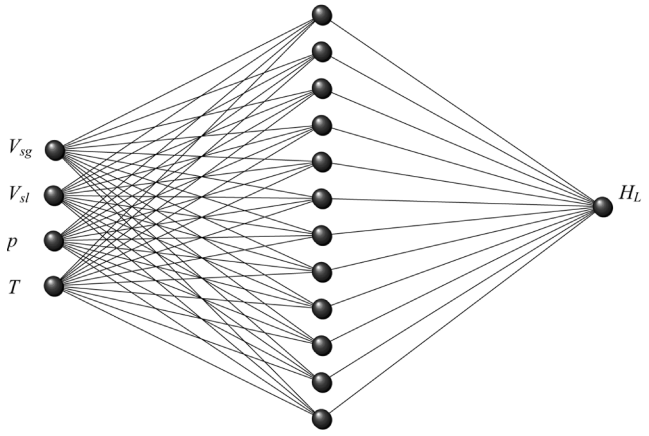

Fig. 3—Location of the experimental data on superficial gas-liquid velocities log-log plot.

TABLE 1—STATISTICAL DESCRIPTION OF THE TRAINING DATA SET (150 DATA POINTS)				
Property	Minimum	Maximum	Average	Standard Deviation
V_{sg}	0.643	160.46	31.385	37.125
V_{sl}	0.007	5.988	0.769	1.116
H_L	0.009	0.606	0.178	0.159
p	28.601	133.30	67.726	26.593
T	76.0	120.02	105.67	9.552

A robust back-propagation gradient descent-learning algorithm was used to train the network. This algorithm uses adaptable learning rates and momentums that adapt themselves during learning. Details of the learning algorithm are found in Appendix A. Training stopped based on mean-square error rather than the classification rate. The resulting weights for the neural network are given in **Table 3.**

Flow-Regime Identification Network. The flow regime's neural network was developed using three layers. The three-layer BPN was designed with 9 input, 50 hidden, and 4 output neurons. Gas and liquid superficial velocities, pressure, average temperature, and liquid holdup were used as input. The output layer consisted of four binary data representing slug, bubble, annular mist, and stratified flow patterns. The training stopped based on classification rate, which is the percent of the correct predictions.

Results and Discussion

Once the neural-network models are trained, they are ready for applications and for predicting the flow regime and holdup, respectively. The following sections discuss the results obtained with 49 data sets not seen by the neural networks during the training process.

Liquid Holdup. To evaluate the accuracy of the developed ANN holdup model, the model was tested using the 49 data sets, which were not seen by the neural networks during training. Most of the existing empirical correlations were used for comparison purposes, including Eaton and Brown,[18] Guzhov *et al.*,[19] Beggs and Brill,[5] Minami and Brill,[20] Brill *et al.*,[21] Gregory *et al.*,[22] Mukherjee and Brill,[23] Hughmark and Pressburg,[24] Hughmark,[25] and Abdul-Majeed.[26] Although some of those correlations[23,24] were developed for vertical flow, they are widely used for horizontal-flow applications.

Several statistical parameters were used in the evaluation, namely, average percent error, E_r; average absolute percent error, E_a; standard deviation, σ; and the correlation coefficient, r. Equations describing these error measures are given in Appendix B, and results of the comparison study are given in **Table 4.**

The developed model outperforms all other correlations. Some empirical correlations performed badly in predicting the holdup values, such those of Guzhov *et al.*,[19] Beggs and Brill,[5] Brill *et al.*,[21] Gregory *et al.*,[22] Hughmark and Pressburg,[24] and Hughmark.[25] The rest of the correlations performed well. Predicted holdup values by those correlations are plotted vs. the corresponding experimental data in **Figs. 5 through 10.** Most of the correlations provided poor predictions for holdup values of less than 0.1. It should be noted that the excellent predictions by the correlations of Minami and Brill[20] and Abdul-Majeed[26] are expected because the data were originally used in developing their correlations. Despite this, the developed neural-network model outperforms all the published correlations in terms of the lowest average percent error (−2.384), the lowest absolute average percent error (9.407), the lowest standard deviation (8.544), and the highest correlation coefficient (0.9896).

Flow Regimes. One objective of this study was to develop an identifying tool to distinguish between different flow regimes in horizontal gas-liquid flow. The flow-regime ANN model developed was tested with 49 data sets. The input parameters were superficial gas and liquid velocities, average pressure and temperature, and liquid holdup. The last parameter could be obtained from the other ANN model. The model perfectly classified the annular flow data (100%) and correctly predicted 98.6% of the stratified flow, 98.5% of the slug flow, and 94.7% of the wave flow. The overall classification rate, the percentage of data cases classified into the correct category, was 98.05%. It is interesting to note that the data not correctly predicted by the ANN model were on the wave/slug and stratified/wave transition zones.

A significance test was performed to evaluate the dependence of the developed model on each of the input parameters. Results indicated that the classification depends strongly on the superficial gas velocity, secondarily on the superficial liquid velocity, and somewhat less on the liquid holdup, average pressure, and temperature (see **Table 5**). This indicated that eliminating the liquid holdup from the input parameters might not result in a big loss of accuracy. To verify that, another similar neural-network model was developed with four input nodes representing gas and liquid superficial velocities and average pressure and temperature. The model perfectly classified the annular flow data (100%) and correctly predicted 97.3% of the stratified flow, 96.9% of the slug flow, and 97.4% of the wave flow. The significance test then was repeated for this model. Results indicated that the classification depends strongly on the superficial gas velocity, secondarily on the superficial liquid velocity, and somewhat less on the average pressure and temperature (see Table 5). The overall classification rate was decreased slightly to 97.56%. It was noted that there is an improvement in predicting wave flow, but the percent of correct predictions decreased from 98.6 to 97.3 for stratified flow and from 98.5 to 96.9 for the slug flow. This time, most of the points that were not predicted correctly lay on stratified/slug transition zone. Thus, the absence of liquid holdup from the input parameters of the ANN model did not strongly affect its accuracy in predicting flow patterns correctly. **Fig. 11** illustrates the flow-pattern predic-

TABLE 2—STATISTICAL DESCRIPTION OF THE TESTING DATA SET (49 DATA POINTS)				
Property	Minimum	Maximum	Average	Standard Deviation
V_{sg}	1.707	54.43	21.953	16.368
V_{sl}	0.019	3.12	0.466	0.703
H_L	0.008	0.435	0.140	0.100
p	43.700	93.70	67.882	17.461
T	82.000	118.0	106.408	8.068

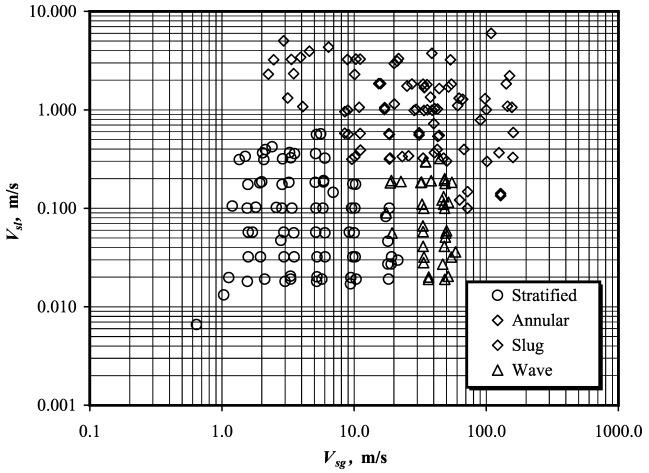

Fig. 4—Schematic of the holdup neural network.

tion for both cases. Also, the perfect prediction of annular flow indicated that the input pattern recognized by the ANN model under annular flow conditions is better correlated and less complex than the pattern for other flows.

Conclusions

1. A new model was developed for predicting the liquid holdup in horizontal gas-liquid flow based on three-layer BPNs. For the test data used in this study, the model outperformed all the existing correlations, providing the lowest error measures and the highest correlation coefficient.
2. A new model was developed for identifying the different flow regimes of horizontal gas-liquid flow. The model was based on three-layer BPNs. Based on the test data used in this study, the model perfectly classifies the annular flow data (100%) and correctly predicts 97.3% of the stratified flow, 96.9% of the slug flow, and 97.4% of the wave flow.
3. Eliminating the liquid holdup from the neural-network inputs resulted in an improvement in predicting wave flow. However, the percent of correct prediction decreased from 98.6 to 97.3 for stratified flow and from 98.5 to 96.9 for the slug flow.
4. Also, the results show that the developed models provide better predictions and a higher accuracy than the empirical correlations developed specifically for these data groups.
5. The developed neural-network models could be improved further by adding more data to the training group to precisely describe the transition between the flow regimes. The developed technique could be applied to inclined and vertical gas-liquid multiphase flow as well.

Nomenclature

a = sigmoid slope, dimensionless
E_a = average absolute percent relative error
E_i = percent relative error
E_r = average percent relative error
H_L = liquid holdup, dimensionless
p = average pressure, psia
r = correlation coefficient
T = average temperature, °F
V_{sg} = superficial gas velocity, ft/s
V_{sl} = superficial liquid velocity, ft/s
σ = standard deviation

Subscripts

exp = experimental
est = estimated

Acknowledgments

The author wishes to thank King Fahd U. of Petroleum and Minerals and the management of the Research Inst. for their support.

References

1. *Two Phase Flow and Heat Transfer,* D. Butterworth and G.F. Hewitt (eds.), Harwell Series, Atomic Energy Research Establishment, Oxford U. Press, London (1979).
2. Brill J.P. and Beggs, H.D.: *Two Phase Flow in Pipes,* U. of Tulsa, Tulsa (1978).
3. Baker, O.: "Design of Pipelines for Simultaneous Flow of Oil and Gas," *Oil and Gas J.* (1953) **53,** No. 12, 185.
4. Scott, D.S.: "Properties of Concurrent Gas-Liquid Flow," *Advances in Chemical Engineering, Vol. 4*, T.B. Drew, J.W. Hoops Jr., and T. Vermulen (eds.), Academic Press, New York City (1963) 200.
5. Beggs, H.D. and Brill J.P.: "A Study of Two-Phase Flow in Inclined Pipes," *JPT* (May 1973) 607.
6. Mandhane, J.M., Gregory, G.A., and Aziz, K.: ''A Flow Map for Gas-Liquid Flow in Horizontal Pipes,'' *Intl. J. of Multiphase Flow* (1986) **12,** No. 4, 711.
7. Taitel, Y. and Dukler, A.E.: "A Model for Predicting Flow Regime Transition in Horizontal and Near Horizontal Gas-Liquid Flow," *AIChE J.* (1976) **22,** No. 1, 47.
8. Cheremisinoff, N.P. and Davis, E.J.: "Stratified Turbulent-Turbulent Gas-Liquid Flow," *AIChE J.* (1979) **25,** No. 1, 48.
9. Shoham, O. and Taitel, Y.: "Stratified Turbulent-Turbulent Gas Liquid Flow in Horizontal and Inclined Pipes," *AIChE J.* (1984) **30,** No. 3, 377.

TABLE 3—NEURAL NETWORK WEIGHTS FOR THE HIDDEN INPUT AND OUTPUT

	V_{sg}	V_{sl}	p	T	Bias	Output
Hidden 1	4.640	24.030	0.229	–0.454	2.179	11.040
Hidden 2	–0.526	–0.453	–1.526	–0.853	–1.860	–0.690
Hidden 3	0.280	–2.865	0.711	–2.149	–0.812	–2.167
Hidden 4	–1.475	–0.857	–1.352	–0.982	–2.341	0.360
Hidden 5	2.332	–6.672	–6.732	3.806	–0.199	–0.267
Hidden 6	–5.436	–3.037	–2.032	–1.553	0.221	3.315
Hidden 7	–3.782	–1.654	–1.245	0.642	–1.586	2.178
Hidden 8	–0.187	–0.159	–1.592	–0.643	–1.871	–1.094
Hidden 9	–1.002	–1.618	–1.807	–1.255	–2.040	0.079
Hidden 10	–0.757	–0.819	–1.364	–0.677	–2.449	–0.190
Hidden 11	–6.341	2.889	0.264	–0.419	–2.125	2.424
Hidden 12	29.87	1.388	–0.699	–0.283	2.666	–16.140
					Bias	4.279

TABLE 4—STATISTICAL RESULTS WITH THE TEST DATA

Correlation	APE	AAPE	Standard Deviation	*r*
Eaton and Brown[18]	–48.346	48.346	21.183	0.9629
Guzhov *et al.*[19]	322.657	324.677	552.169	0.8049
Mukherjee and Brill[23]	–36.189	40.762	33.636	0.9537
Hughmark[25]	62.879	74.443	116.03	0.9396
Hughmark and Presburg[24]	20.958	88.912	140.16	0.9517
Beggs and Brill[5]	– 5.677	25.602	31.533	0.9218
Brill *et al.*[21]	27.286	53.791	91.092	0.8838
Gregory *et al.*[22]	847.38	847.38	968.62	0.7399
Minami and Brill 1[20]	2.762	16.349	22.333	0.9735
Minami and Brill 2[20]	– 3.444	14.501	17.160	0.9741
Abdul-Majeed[26]	1.729	14.559	22.205	0.9730
ANN	– 2.384	9.407	8.544	0.9896

10. Issa, R.I.: "Prediction of Turbulent Stratified Two-Phase Flow in Inclined Pipes and Channels," *Intl. J. of Multiphase Flow* (1988) **14,** No. 2, 141.
11. Dukler, A.E. and Hubbard, M.G.: "A Model For Gas-Liquid Slug Flow In Horizontal And Near Horizontal Tubes," *American Inst. of Chemical Engineering* (1975) **17,** No. 4, 337.
12. Nicholson, K., Aziz, K., and Gregory, G.A.: "Intermittent Two Phase Flow In Horizontal Pipes, Predictive Models," *Can. J. of Chem. Eng.* (1978) **56,** No. 6, 653.
13. Kokal, S.L. and Stanislav, J.F.: "An Experimental Study of Two-Phase Flow in Slightly Inclined Pipes II: Liquid Holdup and Pressure Drop," *Chemical Engineering Science* (1989) **44,** No. 3, 681.
14. Abdul-Majeed, G.H.: " Liquid Slug Holdup in Horizontal and slightly Inclined Two-Phase Slug Flow," *J. Petroleum Science & Technology* (2000) **27,** No. 182, 27.
15. Laurinat, J.E., Hanratty, T.J., and Jepson, W.P.: "Film Thickness Distribution for Gas-Liquid Annular Flow in a Horizontal Pipe," *Intl. J. of Multiphase Flow* (1985) **6,** No. 112, 179.
16. James, P.W. *et al.:* "Developments in the Modeling of Horizontal Annular Two-Phase Flow," *Intl. J. of Multiphase Flow* (1987) **13,** 173.
17. Wallis, G.B.: *One Dimensional Two-Phase Flow,* McGraw-Hill, New York City (1969).
18. Eaton, B.A. and Brown, K.E.: "The Prediction of Flow Patterns, Liquid Holdup and Pressure Losses Occurring During Continuous Two-Phase Flow In Horizontal Pipelines," *JPT* (June 1967) 815; *Trans.*, AIME, **240.**
19. Guzhov, A.I., Mamayev, V.A., and Odishariya, G.E.: "A Study of Transportation in Gas-Liquid Systems," *Proc.*, 10th Intl. Gas Conference, Hamburg, West Germany (1967).
20. Minami, K. and Brill, J.P.: "Liquid Holdup in Wet-Gas Pipelines," *SPEPE* (February 1987) 36.
21. Brill, J.P. *et al.:* "Analysis of Two-Phase Tests in Large-Diameter Flow Lines in Prudhoe Bay Field," *SPEJ* (June 1981) 363; *Trans.*, AIME, **271.**
22. Gregory, G.A., Nicholson, M.K., and Aziz, K.: "Correlation of the Liquid Volume Fraction in the Slug for Horizontal Gas-Liquid Slug Flow," *Intl. J. of Multiphase Flow* (1978) **4,** No. 1, 33.
23. Mukherjee, H. and. Brill, J.P.: "Liquid Holdup Correlations for Inclined Two-Phase Flow," *JPT* (May 1983) 1003; *Trans.*, AIME, **275.**
24. Hughmark, G.A., and Presburg, B.S.: "Holdup and Pressure Drop with Gas Liquid Flow in a Vertical Pipe," *AIChE J.* (1961) **7,** No. 4, 677.
25. Hughmark, G.A.: "Holdup in Gas-Liquid Flow," *Chemical Engineering Progress* (1962) **58,** No. 1, 62.
26. Abdul-Majeed, G.H.: "Liquid Holdup Correlations for Horizontal, Vertical and Inclined Two-Phase Flow," paper SPE 26279 available from SPE, Richardson, Texas (1993).
27. Abdul-Majeed, G.H.: "Liquid Slug Holdup in Horizontal Two-Phase Gas-Liquid Flow," *J. of Petroleum Science & Technology* (1996) **15,** Nos. 3 and 4, 271.
28. Xiao, J.J., Shoham, O., and Brill, J.P.: "A Comprehensive Mechanistic Model for Two-Phase Flow in Pipelines," paper SPE 20631 presented at the 1990 SPE Annual Technical Conference and Exhibition, New Orleans, 23–26 September.
29. Baker, A., Nilsen, K., and Gabb, A.: "Pressure Loss, Liquid Holdup Calculations Developed," *Oil & Gas J.* (1988) **11,** 55.
30. Gomez, L.E. *et al.:* "A Unified Mechanistic Model for Steady-State Two-Phase Flow in Wellbores and Pipelines," paper SPE 56520 pre-

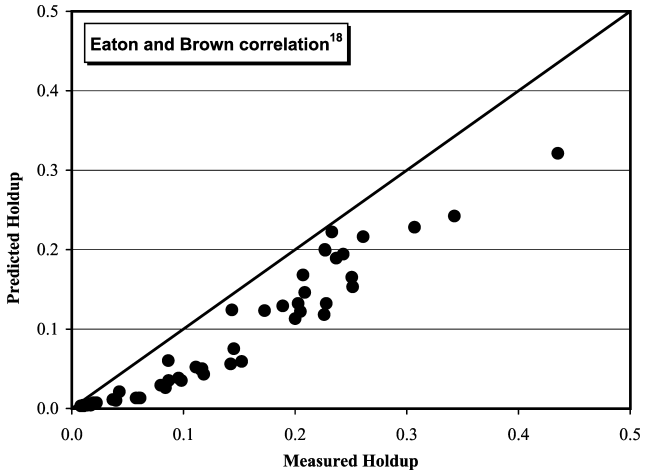

Fig. 5—Crossplot of Eaton and Brown correlation.[18]

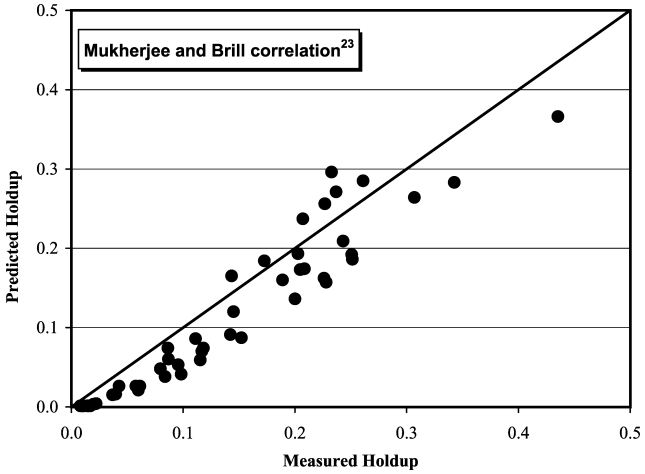

Fig. 6—Crossplot of Mukherjee and Brill correlation.[23]

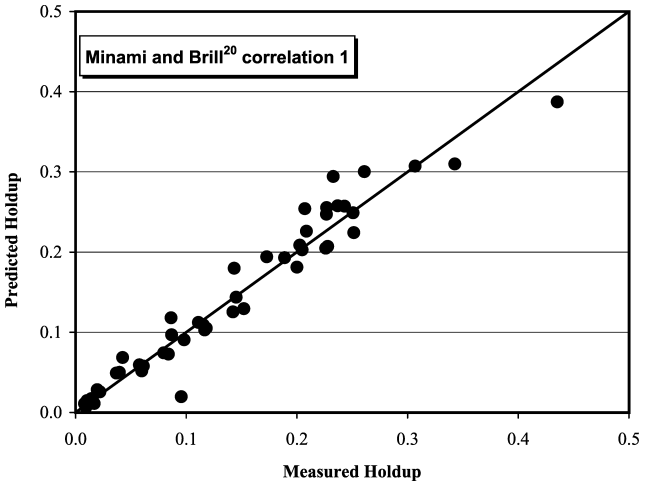

Fig. 7—Crossplot of Minami and Brill correlation 1.[20]

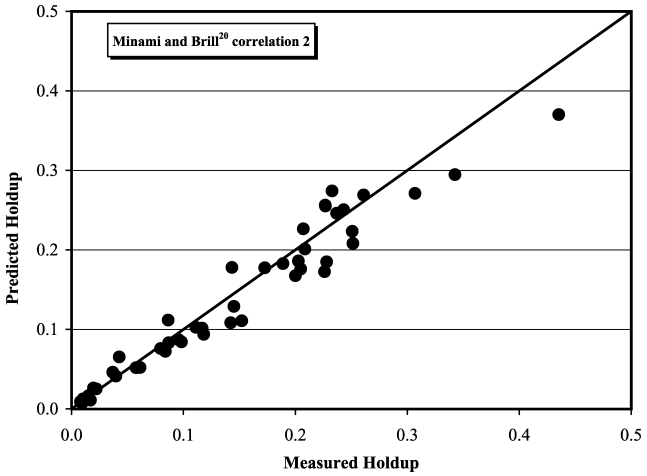

Fig. 8—Crossplot of Minami and Brill correlation 2.[20]

sented at the 1999 SPE Annual Technical Conference and Exhibition, Houston, 3–6 October.

31. Mohaghegh, S.: "Virtual-Intelligence Applications in Petroleum Engineering: Part 1—Artificial Neural Networks," *JPT* (September 2000) 64.
32. van der Spek, A. and Thomas, A.: "Neural-Net Identification of Flow Regime With Band Spectra of Flow-Generated Sound," *SPEREE* (December 1999) 489.
33. Ternyik, J., Bilgesu, H.I., and Mohaghegh, S.: "Virtual Measurement in Pipes: Part 2—Liquid Holdup and Flow Pattern Correlations," paper SPE 30976 presented at the 1995 Eastern Regional Meeting, Morgantown, West Virginia, 17–21 September.
34. Bishop, C.: *Neural Networks for Pattern Recognition,* Oxford U. Press, New York City (1995).
35. Fauset, L.: *Fundamentals of Neural Networks,* Prentice Hall, New Jersey (1996).
36. Hornik, K.: "Multilayer Feedforward Networks are Universal Approximators," *Neural Networks* (1989) **2,** No. 5, 359.
37. Varotsis, N. *et al.:* "A Novel Non-Iterative Method for the Prediction of the PVT Behavior of Reservoir Fluids," paper SPE 56745 presented at the 1999 SPE Annual Technical Conference and Exhibition, Houston, 3–6 October.
38. Abdel-Wahhab, O. and Sid-Ahmed, M.A.: "A New Scheme for Training Feedforward Neural Networks," *Pattern Recognition* (1997) **30,** No. 3, 519.

Appendix A—Training Algorithm Used in This Study

The training algorithm used in this study was originally proposed by Abdel-Wahhab and Sid Ahmed.[38] This algorithm is shown to be faster and more stable than other schemes presented in the literature and is summarized here. Fig. 10 in Ref. 38 is used for notations.

1. Initialization.
   - Randomize all weights in the network.
   - For layers $j = 1$ through L, initialize the $m_j \times m_j$ matrices $\boldsymbol{S}_j$ by a small, nonzero, random number, in which $m_j =$ the length of the vectors $\boldsymbol{x}_{j-1}$.
   - Equate the node offsets $\boldsymbol{x}_{j-1,0}$ of every node to some nonzero constant for layers $j = 1$ through L.

2. Choose a training pattern.
   - Randomly select an input/output pair $(\boldsymbol{x}_0, \boldsymbol{o})$ to present to the network.
   - For each layer j and for every node k, calculate the summation output:

$$y_{jk} = \sum_{i=0}^{N} (x_{j-1,i} \times w_{jki}), \quad \text{(A-1)}$$

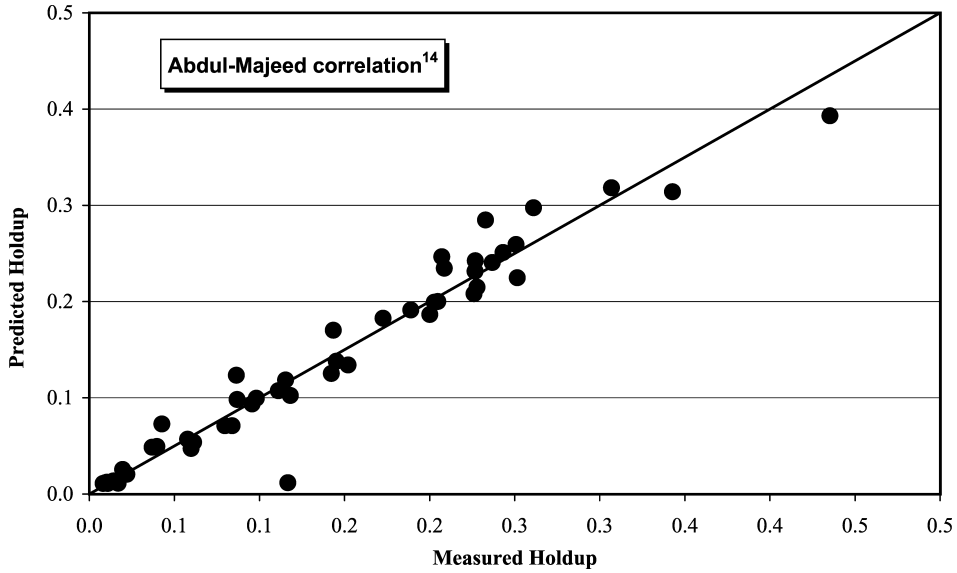

Fig. 9—Crossplot of Abdul-Majeed correlation.

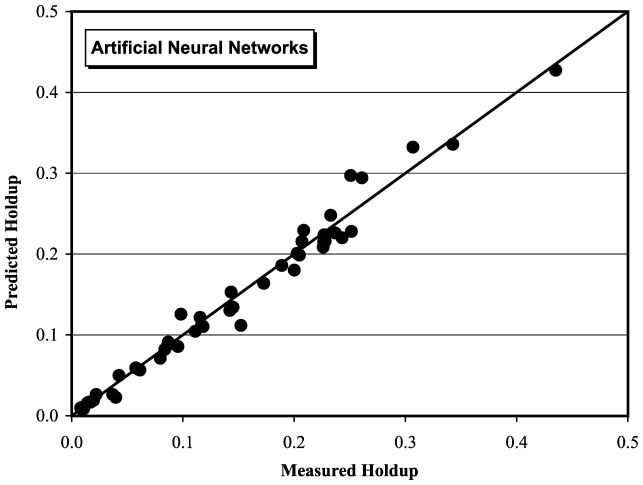

Fig. 10—Crossplot of an ANN model.

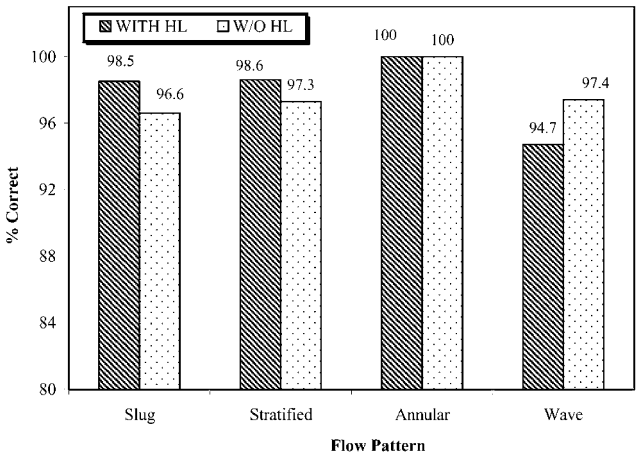

Fig. 11—Comparison of flow pattern prediction with and without holdup as an input.

the function output:

$$f(y_{jk}) = \frac{[1 - \exp(-a \cdot y_{jk})]}{[1 + \exp(-a \cdot y_{jk})]}, \quad \text{(A-2)}$$

and the derivative of $f(y_{jk})$:

$$f'(y_{jk}) = \frac{2a \cdot \exp(-a \cdot y_{jk})}{[1 + \exp(-a \cdot y_{jk})]^2}. \quad \text{(A-3)}$$

Here, N = the number of inputs to a node, and the constant a = the sigmoid slope.

3. Invoke the unweighted gain equations.

• For each layer j from 1 through L, the predicted residual variance inverse is given by

$$\sigma_j = \frac{1}{[(\boldsymbol{x}_j \boldsymbol{S}_j)^T (\boldsymbol{x}_j \boldsymbol{S}_j) + b_j]}. \quad \text{(A-4)}$$

• The unweighted Kalman gain is given by

$$\boldsymbol{k}_j = \boldsymbol{S}_j (\boldsymbol{x}_j \boldsymbol{S}_j). \quad \text{(A-5)}$$

4. Update the inverse matrix.

• Calculate:

$$\boldsymbol{S}_{j+1} = \frac{\boldsymbol{S}_j - (\gamma_j \boldsymbol{k}_j)(\boldsymbol{x}_j \boldsymbol{S}_j)^T}{b_j}, \quad \text{(A-6)}$$

$$\text{in which } \gamma_j = \frac{\sigma_j}{1 + \sqrt{\sigma_j}}. \quad \text{(A-7)}$$

5. Back-propagate error signals.

• Calculate error signals for every node k.

$$e_{Lk} = f'(y_{Lk})\,(o_k - x_{Lk}) \text{ for the output layer, } L. \quad \text{(A-8)}$$

TABLE 5—SIGNIFICANCE TEST RESULTS FOR THE FLOW PATTERN MODEL

	% Correct	Difference	% Correct	Difference
All	98.537		98.049	
V_{sg}	59.024	–39.512	60.488	–37.561
V_{sl}	68.780	–29.756	63.415	–34.634
p	84.878	–13.659	80.976	–17.073
T	80.976	–17.561	88.293	–9.7561
H_L	82.927	–15.610		

$$e_{jk} = f'(y_{jk}) \sum_i (e_{j+1,i} w_{j+1,i,k}) \text{ for the hidden layers from } L\text{-1 to 1.} \quad \text{(A-9)}$$

6. Find the desired summation output.

• For every node k, in the output layer, calculate the desired summation output with the inverse function.

$$d_k = \frac{1}{a} \ln \frac{1 + o_k}{1 - o_k}. \quad \text{(A-10)}$$

7. Update the weights.

For every node k, the weight vectors in the output layer L are updated by

$$\boldsymbol{w}_{Lk} = \boldsymbol{w}_{Lk} + \boldsymbol{k}_L (\boldsymbol{d}_k - \boldsymbol{y}_{Lk}), \quad \text{(A-11)}$$

and for each hidden layer $j = 1$ through L–1, weight vectors are updated by

$$\boldsymbol{w}_{jk} = \boldsymbol{w}_{jk} + \boldsymbol{k}_j \boldsymbol{e}_{jk} \mu_j. \quad \text{(A-12)}$$

8. Stopping criteria.

• Use the mean-square error of the network output as a convergence test.

• Run the algorithm for a fixed number of iterations.

• Split the data into two sets: one set to train the network and the other set to test the error.

This method is called cross validation. It gives the ability to monitor the generalization performance of the network and to prevent the network from overfitting the training data.

Appendix B—Statistical Error Analysis

To compare the performance and accuracy of the new model to other empirical correlations, statistical error analysis is performed. The statistical parameters used for comparison are: average percent relative error, average absolute percent relative error, minimum and maximum absolute percent error, root mean square, and the correlation coefficient. Equations for those parameters are given here.

1. Average percent relative error.

This is the measure of the relative deviation from the experimental data, defined by

$$E_r = \frac{1}{n} \sum_{i=1}^{n} |E_i|, \quad \text{(B-1)}$$

in which E_i = the relative deviation of an estimated value from an experimental value.

$$E_i = \left[\frac{(H_L)_{exp} - (H_L)_{est}}{(HL)_{exp}} \right] \times 100 \; i = 1,2, ...n. \; . . . . . \text{(B-2)}$$

2. Absolute average percent relative error.
This error measures the relative absolute deviation from the experimental values, defined by

$$E_a = \frac{1}{n} \sum_{i=1}^{n} |E_i|. \; . . . . . \text{(B-3)}$$

3. Standard deviation.
The standard deviation is a measure of how widely values are dispersed from the average value (the mean). Standard deviation is based on the entire population and is given as arguments. The standard deviation is calculated with the "biased" or "*n*" method, defined by

$$\sigma = \left[\frac{n \sum_{i=1}^{n} (E_i)^2 - (\sum_{i=1}^{n} E_i)^2}{n^2} \right]^{1/2} \; . . . . . \text{(B-4)}$$

4. The correlation coefficient.
Defined by Eq. B-5, this represents the degree of success in reducing the standard deviation by regression analysis.

$$r = \sqrt{1 - \sum_{i=1}^{n} [(H_L)_{exp} - (H_L)_{est}]_i^2 \; / \; \sum_{i=1}^{n} [(H_L)_{exp} - \overline{H}_L]}, \; . . . . . \text{(B–5)}$$

in which $\overline{H}_L = \frac{1}{n} \sum_{i=1}^{n} [(H_L)_{exp}]_i$. . . . . (B-6)

SI Metric Conversion Factors

ft × 3.048*	E–01	= m
°F (°F–32)/1.8		= °C
in. × 2.54*	E+00	= cm
psi × 6.894 757	E+00	= kPa

*Conversion factor is exact.

El-Sayed A. Osman is a research engineer in the Center for Petroleum and Minerals of the Research Inst., King Fahd U. of Petroleum and Minerals (KFUPM), Dhahran, Saudi Arabia. e-mail: saosman@kfupm.edu.sa. His research interests include sand control, reservoir simulation, and artificial intelligence applications in petroleum engineering. Osman holds BS and MS degrees from Cairo U. and a PhD degree from KFUPM, all in petroleum engineering.